

## Removal of Pb (II) from an Aqueous Solution Using Modified Cuttlebone as a Biosorbent

Pathompong Vibhatabandhu<sup>a</sup> and Sarawut Srithongouthai<sup>b</sup>

<sup>a</sup> Program in Biotechnology, Faculty of Science, Chulalongkorn University, Bangkok, Thailand

<sup>b</sup> Department of Environmental Science, Faculty of Science, Chulalongkorn University, Bangkok, Thailand

---

### Abstract

Biosorption is a promising method for removing heavy metals from wastewater, evidenced by several studies on the high efficiency and cost-effectiveness of its practical usage. In the present study, cuttlebone powder (CB-P) and cuttlebone modified via carbonization at 400°C (CB-M400) were used to remove Pb (II) from an aqueous solution. The adsorbents were characterized using a scanning electron microscope (SEM) and an X-ray diffractometer. An adsorption study was carried out at different initial pHs, biosorbent doses, and initial Pb (II) concentrations, in batch experiments in order to evaluate the optimum conditions for Pb (II) removal. The results showed that CB-P obtained a larger specific surface area (8.41 m<sup>2</sup>/g) than CB-M400 (2.69 m<sup>2</sup>/g); however, the calcite in CB-M400 displayed a remarkably higher sorption capacity for Pb (II) than the aragonite in CB-P. The carbonization of organic matter in CB-P resulted in a higher calcium carbonate content and the formation of fixed carbon, increasing the adsorption capacity of CB-M400. Optimum conditions for removal of Pb (II) occurred at pH 4.0 with 0.2 g/L of the biosorbent dose. In an equilibrium study, Langmuir's isotherm was fixed at  $R^2 > 0.9$ ; the maximum capacities were calculated to be 869.57 mg/g for CB-P and 1,573.56 mg/g for CB-M400. In a kinetic study, a pseudo second-order model was fixed; the higher adsorption rate was found in CB-M400.

**Keyword:** Pb (II) removal; biosorption; cuttlebone; modification

---

### 1. Introduction

Heavy metals contamination has become a serious environmental issue worldwide; their bioaccumulation and biomagnification via the ecological food chain causes toxicity and increases health risks in the human population (Baby *et al.*, 2010). Anthropogenic activity is one of the major sources of heavy metals contamination. Pb in wastewater and sludge is particularly problematic, a waste product created from several industries such as metallic electroplating, radiation manufacturing, and battery storage (Kadirvelu *et al.*, 2001; Khalid and Rahman, 2010). Pb mainly accumulates in the bones, brain, kidneys, and muscles, causing anemia, kidney disease, nervous disorders, and even death (Mudhoo *et al.*, 2012).

Adsorption is now recognized as an effective and economic way to treat heavy metal wastewater due to its flexibility in implementation, high-quality treatment outcomes, and partial regeneration through the desorption process (Fu and Wang, 2011). Using biosorption or a naturally occurring abundant biological material as an adsorbent is another method for removing heavy metals (Bailey *et al.*, 1999; Fu

and Wang, 2011). Moreover, the physical and chemical modification of biomass can solve problems caused by the non-purity components of biomass and accrued capability of adsorbents (Wan Ngah and Hanafiah, 2008). Various types of materials have been investigated for their ability to remove heavy metals such as cadmium, arsenic, and lead (Yadanaparthi *et al.*, 2009). Algal biomass (Bulgariu and Bulgariu, 2012; Ibrahim, 2011; Yalçin *et al.*, 2012), plant biomass (Tang *et al.*, 2013; Hassan and Kaewsichan, 2016), eggshells (Vijayaraghavan and Joshi, 2013), and crab shells (Lee *et al.*, 1997; Ramalingam *et al.*, 2014) are some examples of alternative biosorbents used for lead removal; they are naturally abundant biomaterials, renewable resources, and waste products.

The cuttlebone (cuttlefish bones or *os sepiæ*) is the internal skeleton of the cuttlefish (*Sepia officinalis*), which is common in coastal regions. The cuttlebone is a waste byproduct of processing cuttlefish; it is commonly used in traditional medicine or as a calcium-rich dietary supplement. Natural CaCO<sub>3</sub> usually exists in calcite (trigonal crystal) and aragonite (orthorhombic crystal). Geological CaCO<sub>3</sub> has the ability to adsorb a certain amount of heavy metals from aqueous solutions (Du *et al.*, 2011). As the main source

of biogenic  $\text{CaCO}_3$ , cuttlebone is comprised of  $\text{CaCO}_3$  (89-94%), protein (3-7%), and  $\beta$ -chitin (3-4%) (Birchall and Thomas, 1983; Klungsuwan *et al.*, 2013). Recently, researchers have found that cuttlebone can be used as a biosorbent for the removal of heavy metals from aqueous solutions (Ben Nasr *et al.*, 2011; Li *et al.*, 2010; Sandesh *et al.*, 2013). However, little research has been conducted on the sorption of heavy metals by modified biogenic carbonate. According to the literature review, conventional pyrolysis (carbonization) is an efficient way to create a large surface area on biochar, which might increase its adsorption efficiency (Boonamnuyvitaya *et al.*, 2004; Chen *et al.*, 2011; Wang *et al.*, 2008).

In the present study, cuttlebones were made into two forms of biosorbents: cuttlebone powder (CB-P) and cuttlebone modified with carbonization at  $400^\circ\text{C}$  (CB-M400). This was done in order to study the removal of Pb (II) from an aqueous solution. The effects of initial pH, sorbent dosage, and initial concentration were studied in order to determine the optimum conditions for Pb (II) removal. The sorption isotherms and kinetics of CB-P and CB-M400 were also investigated in order to understand the equilibrium and mechanisms of biosorbents for removing Pb (II) from an aqueous solution.

## 2. Experimental Methods

### 2.1 Biosorbent preparation and characterization

The cuttlebones were naturally occurring and were collected from the Lamchareon and Maerumpueng seacoasts in the Rayong province of Thailand. The cuttlebones were washed and oven-dried at  $80^\circ\text{C}$ , then crushed and sieved to a particle size  $< 106 \mu\text{m}$  (Endecotts; England). CB-P was rinsed with distilled water and dried at  $60$ - $80^\circ\text{C}$  for later use. CB-M400 was prepared via carbonization of the cuttlebone powder ( $< 106 \mu\text{m}$ ) at  $400^\circ\text{C}$  for two hours in a furnace (Nabertherm, LT 15/12; Germany). All adsorbents used in this study were oven-dried at  $60$ - $80^\circ\text{C}$  and cooled in a desiccator before experimentation.

The surface characterization of CB-P and CB-M400 before and after Pb (II) adsorption was analyzed via scanning electron microscope (SEM) with an energy dispersive spectrometer attachment (SEM-EDS) (JEOL, JSM-6610LV, Link ISIS Series 300; USA). The chemical crystal structures of the adsorbents were qualitatively and quantitatively analyzed via X-ray diffractometer (Bruker AXS, Diffractometer D8; Germany).

### 2.2 Pb (II) adsorption experiment

All of the treatments were carried out in three replications using batch experiments. The aqueous solution was prepared by diluting the stock  $\text{Pb}(\text{NO}_3)_2$  in  $\text{HNO}_3$  (0.5 M). The adsorption experiment was conducted by mixing the aqueous solution of Pb (II) with a fixed dose of biosorbents (CB-P and CB-M400) at fixed time intervals in acid-washed glassware and then separated from the aqueous solution by filtration. The Pb (II) concentrations in the aqueous solution without adsorbents and the separated aqueous solution after adsorption were analyzed as the initial and final Pb (II) concentrations using an atomic absorption spectrophotometer (Agilent, 240AA). The adsorption capacity,  $q$  (mg/g) and the adsorption efficiency (%) were used to compare the quantity of Pb adsorption (Equations 1 and 2).

$$\text{Adsorption capacity, } q \text{ (mg/g)} = \frac{(C_i - C_f)}{S} \quad (1)$$

$$\text{Adsorption Efficiency (\%)} = \frac{(C_i - C_f)}{C_i} \times 100 \quad (2)$$

where  $C_i$  and  $C_f$  are the initial and final Pb (II) concentrations (mg/L), respectively, and  $S$  is the concentration of adsorbent in the mixing solution (g/L).

The effects of initial pH level (1-5), biosorbent dose (0.1-0.7 g/L), and initial Pb (II) concentration (10-1000 mg/L) were investigated in terms of difference values via refrigerated orbital incubator with a shaking speed of 100 rpm at  $30^\circ\text{C}$  (SANYO GALLenkamp PLC, IOC400.XX2.C).

### 2.3 Adsorption isotherm

The adsorption equilibrium was analyzed via Langmuir's and Freundlich's adsorption isotherms (Equations 3 and 4, respectively).

$$\frac{C_e}{q_e} = \frac{1}{K_L q_m} + \frac{C_e}{q_m} \quad (3)$$

$$\log q_e = \log K_F + \frac{1}{n} \log C_e \quad (4)$$

where  $C_e$  is the Pb (II) concentration at the equilibrium of adsorption (mg/L);  $q_e$  is the amount of adsorption equilibrium (mg/g);  $K_L$  and  $K_F$  are Langmuir's and Freundlich's isotherm constants, respectively;  $q_m$  is the maximum adsorption capacity (mg/g) of Langmuir's isotherm; and  $n$  is the adsorption intensity of Freundlich's isotherm.

## 2.4 Adsorption kinetic

The optimum adsorbent dose was added to 1 L of 100 mg/L and 1 L of 500 mg/L of Pb (II) aqueous solution with an optimum pH at 30°C and mixed with a 200 rpm magnetic stirrer bar. At different time intervals, 1 mL from the solution was removed and filtrated with a syringe filter with a pore size of 0.45  $\mu\text{m}$  (Advantec, 25CS045AN); the Pb (II) concentration of the solution was then analyzed. The pseudo first-order and pseudo second-order adsorption kinetic models were determined using Equations 5 and 6.

$$\log(q_e - q_t) = \log q_e - \frac{k_1}{2.303} t \quad (5)$$

$$\frac{t}{q_t} = \frac{1}{k_2 q_e^2} - \frac{1}{q_e} t \quad (6)$$

where  $q_e$  (mg/g) is the adsorption capacity at equilibrium,  $q_t$  is the amount of metal adsorbed (mg/g) at time  $t$  (min),  $k_1$  is the pseudo first-order equilibrium rate constant (1/min), and  $k_2$  is the pseudo second-order equilibrium rate constant (g/mg/min).

## 3. Results and Discussion

### 3.1 Biosorbent characteristics

The white powder of the CB-P and the black powder of the CB-M400 surface structures as well as the elements of both biosorbent surfaces were characterized and identified via SEM-EDS. Fig. 1 shows the SEM

images of the biosorbent surfaces before Pb (II) adsorption at 3500x and 10000x magnification. Microsized and nanosized pores were observed in both CB-P (Fig. 1(A)) and CB-M400 (Fig. 1(B)). As identified by SEM-EDS, elements on the adsorbent surfaces (shown in Table 1) before Pb (II) adsorption and elements in CB-P and CB-M400 showed similar contents: they were rich in Ca, C, and O; further, the crystals in the Pb compounds could be seen clearly on the surface of both biosorbents after Pb (II) adsorption testing (Fig. 2(A) and 2(B)).

The crystalline structures of the adsorbents before and after Pb (II) adsorption were confirmed using X-ray powder diffraction (XRD). The XRD patterns (data not shown) and quantity of each crystalline structure (Table 2) displayed the  $\text{CaCO}_3$  aragonite crystals. These were major components in CB-P, where as only calcite was detected in CB-M400. Take-up Pb (II) adsorbents were identified as follows:  $\text{PbCO}_3$  and  $\text{Pb}_3(\text{CO}_3)_2(\text{OH})_2$ , with aragonite in CB-P and calcite in CB-M400.

The main components in CB-P were the aragonite and  $\text{CaCO}_3$  crystals as well as crystals from an organic component that coated the inorganic matter, appearing as a thin, corrugated film (Birchall and Thomas, 1983). The structure and components of CB-M400 were affected by the heat of the CB-P carbonization process. In the  $\text{CaCO}_3$  component, the aragonite structure was thermally transformed into calcite at 407-550°C (Florek *et al.*, 2009; Klungsuwan *et al.*, 2013; Li *et al.*,

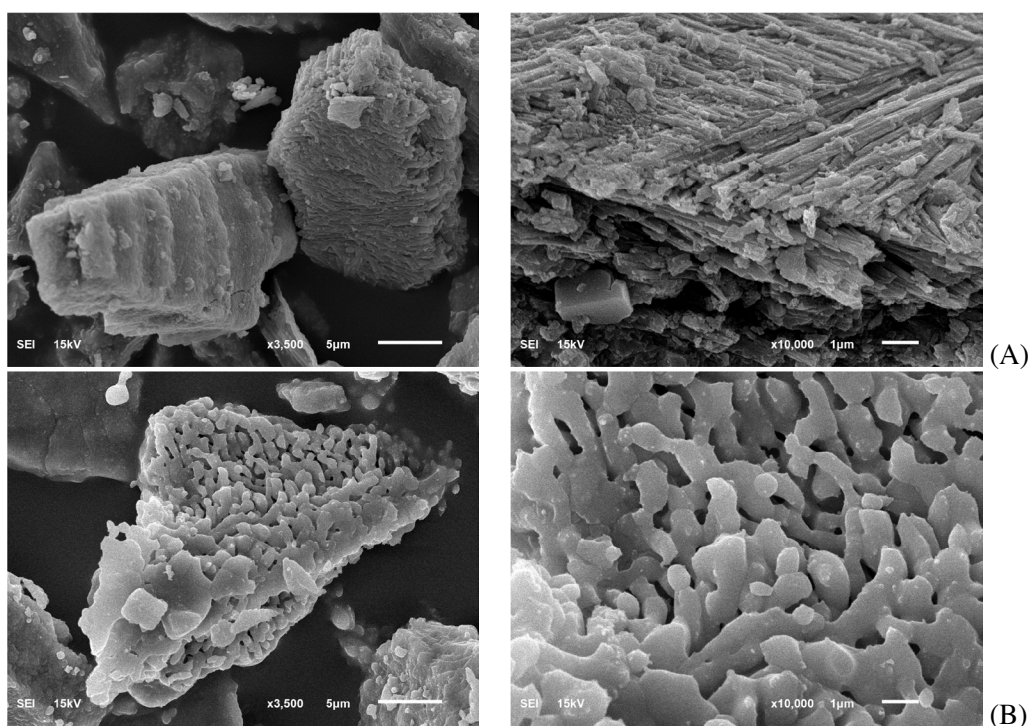


Figure 1. Surface characterization of biosorbents before Pb (II) adsorption of (A) CB-P and (B) CB-M400 at a magnification of 3500x (left) and 10000x (right) using SEM-EDS



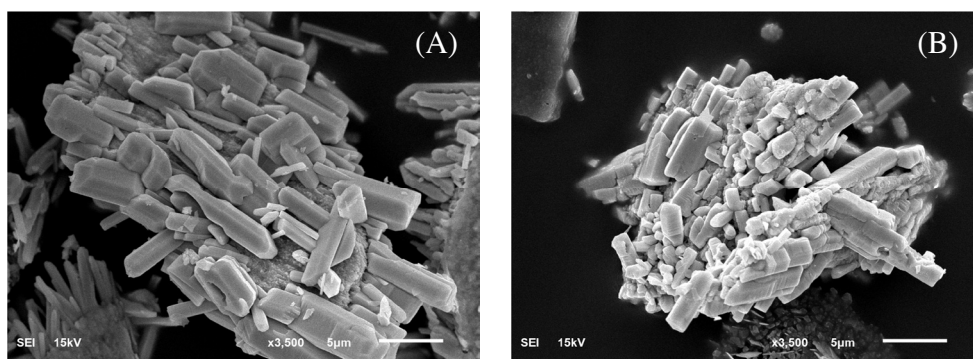


Figure 2. Surface characterization of (A) CB-P and (B) CB-M400 after Pb (II) adsorption at a magnification of 3500x using SEM-EDS

2015). Thermal degradation in the absence of oxygen produces inorganic charcoal from organic matter (Demirbas and Arin, 2002). In this study, the percentage of the carbon weight of the biosorbents decreased from 25.02% in CB-P to 16.33% in CB-M400; the percentage of the calcium weight showing the  $\text{CaCO}_3$  content increased from 21.83% in CB-P to 31.90% in CB-M400 (Table 1) as a result of the degradation of the organic carbon in CB-P; it transformed into fixed carbon after carbonization.

$\text{PbCO}_3$  and  $\text{Pb}_3(\text{CO}_3)_2(\text{OH})_2$  crystals were found on the biosorbent surfaces after Pb (II) adsorption; these results are supported by the Pb precipitation via  $\text{CO}_3^{2-}$  found in crab shell adsorbents (Lee *et al.*, 1997). The dissolution of  $\text{CaCO}_3$  formed  $\text{CO}_3^{2-}$  and  $\text{HCO}_3^-$  in the solution; these reacted with Pb in the solution to become  $\text{PbCO}_3$  and  $\text{Pb}_3(\text{CO}_3)_2(\text{OH})_2$ , respectively, which were precipitated and adsorbed on the surface. Small amounts of chitin and organic protein from the cuttlebone in CB-P and fixed carbon content in CB-M400 were detected, emphasizing the function of chelates in the adsorption of Pb precipitate compounds.

### 3.2 Effect of pH

The pH of the aqueous solution plays an important role in the sorption process because it affects the complexation reaction, electrostatic interaction, and precipitation between the heavy metal ions and the sorbents (Du *et al.*, 2011). Fig. 3(A) illustrates the effect of pH on Pb (II) adsorption's capacity and efficiency, the values of which shared the same trend with a pH of 1.0-2.0, increasing with a pH of 3.0-4.0 and changing little at a pH of 5.0. The results indicate that the solution's pH strongly affected the Pb (II) adsorption of CB-P and CB-M400. This may be due to the protonation on the biosorbent surface, which neutralized binding at the active sites (Ibrahim, 2011). In particular, the dissolution of  $\text{CaCO}_3$  in cuttlebone can decrease its biosorbent properties, resulting in a non-effective adsorbent in Pb (II) removal. The higher adsorption efficiency of CB-M400 at a pH of 1.0-2.0 was possible due to a higher  $\text{CaCO}_3$  content and the function of fixed carbon. Fig. 3(B) demonstrates a changed pH value after the adsorption process ( $\Delta\text{pH}$ ) expresses

Table 1. Element on adsorbent surface before and after adsorbed Pb (II) using SEM-EDS

Element	Before Pb (II) adsorption (%)		*After Pb (II) adsorption (%)	
	CB-P	CB-M400	CB-P	CB-M400
C	25.02	16.33	17.80	16.10
O	51.66	49.89	9.89	17.32
Na	0.77	1.03	-	-
Mg	-	0.62	-	-
Cl	0.73	0.24	-	-
Ca	21.83	31.90	1.80	1.26
Pb	-	-	70.50	65.32

\* using aqueous solution with Pb (II) of 500 mg/L, at pH of 4.0, with an adsorbent dose of 0.2 g/L, for 360 minutes at 30°C

Table 2. Quantitative analysis of crystalline in CB-P and CB-M400 using XRD

Crystalline	Before Pb (II) adsorption (%)		*After Pb (II) adsorption (%)	
	CB-P	CB-M400	CB-P	CB-M400
CaCO <sub>3</sub> (Aragonite)	98.93	-	23.92	-
CaCO <sub>3</sub> (Calcite)	0.74	100.00	-	31.20
NaCl	2.34	-	-	-
PbCO <sub>3</sub>	-	-	74.84	67.52
Pb <sub>3</sub> (CO <sub>3</sub> ) <sub>2</sub> (OH) <sub>2</sub>	-	-	1.24	1.29

\* using aqueous solution with Pb (II) of 500 mg/L, at pH of 4.0, with an adsorbent dose of 0.2 g/L, for 360 minutes at 30°C

the removal of H<sup>+</sup> from the solution. While the initial pH is 1.0, a high concentration of H<sup>+</sup> produces H<sub>2</sub>CO<sub>3</sub> and then shifts to CO<sub>2</sub>; some of this is adsorbed on non-CaCO<sub>3</sub> contents, with the result that the pH is slightly increased and less ΔpH occurs. For an initial pH of 2.0 and 3.0, the system balance of H<sup>+</sup> with CO<sub>3</sub><sup>2-</sup> reacts to HCO<sub>3</sub><sup>-</sup> and H<sub>2</sub>CO<sub>3</sub>, increasing the ΔpH. A higher ΔpH in CB-M400 caused the greater CaCO<sub>3</sub> content in CB-M400, which was more dissolved than CB-P. With an initial pH of 4.0 and 5.0, resistant pH-changing buffer properties of CO<sub>3</sub><sup>2-</sup>, HCO<sub>3</sub><sup>-</sup>, and H<sub>2</sub>CO<sub>3</sub> equilibrium occurs as the ΔpH decreases and the final pH changes slightly. In divalent heavy metal ion adsorption studies, the effect of pH on adsorption has the same pattern of a peak at the pH

value range of 4.0-5.0 due to hydronium ion completion in low pH and metal hydroxide precipitation in high pH (Bulgariu and Bulgariu, 2012; Chen *et al.*, 2011; Ibrahim, 2011; Tang *et al.*, 2013; Vijayaraghavan and Joshi, 2013). The Pb (II) uptake efficiencies at pH 4.0 and 5.0 were not different between pH values in the CB-P and CB-M400 treatments. As can be seen in the industrial effluent characteristic index, most contaminated heavy metal wastewater has a low pH value (Kadirvelu *et al.*, 2001; Khalid and Rahman, 2010); therefore, the biosorbents from this study are suitable for practical applications. In future experiments, an aqueous solution with a pH of 4.0 will be used for further characterization.

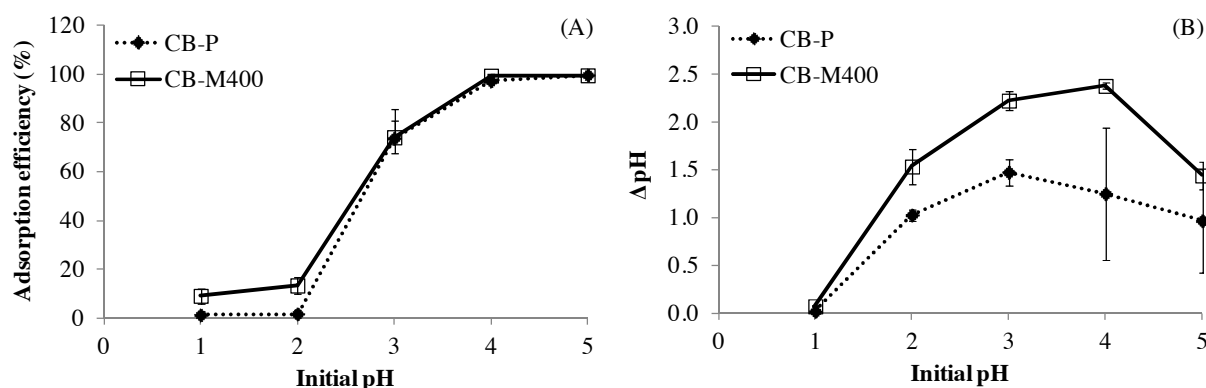


Figure 3. (A) represents the effect of pH on the Pb(II) adsorption efficiency of CB-P and CB-M400 with an initial Pb (II) concentration of 500 mg/L, a biosorbent dose of 0.5 g/L, and a contact time of 240 min. (B) represents the changed pH value after the adsorption process (ΔpH)

### 3.3 Effect of adsorbent and Pb (II) concentration

Dosage is an important factor that determines how much sorbent is required to remove a specific amount of metal ions from the solution completely. Dosage is an important factor in determining how much sorbent is required to completely remove a specific amount of metal ions from the solution. The effects of the biosorbent dosage (0.2-0.7 g/L) and the Pb(II) concentration (10-1000 mg/L) on adsorption capacity and efficiency were tested at the optimum initial pH (4.0); the results are presented in Fig. 4. The capacity and efficiency of CB-P and CB-M400 showed similar response patterns, whereas higher capacity was observed in CB-M400. In the low initial concentrations of Pb (II) (10 mg/L and 100 mg/L), 100% of Pb (II) were removed

even though not all of the adsorbent was available at the active sites that were binding metal ions; this resulted in a reduced capacity when more adsorbent was added. In contrast, some of Pb (II) were not removed in the higher concentrations of Pb (II) (250 mg/L and 500 mg/L); the adsorption capacity increased, peaking at 0.2 g/L. This may explain why a higher dose of adsorbent correlates to the greater availability of active sites for the ions and why the aggregation of intense adsorbent decreases the amount of effective surface area (Ibrahim, 2011). At the extreme high concentration at 1000 mg/L, the capacity in each adsorbent dosage did not differ or only slightly inversely decreased the adsorbent dosage; the capacity of CB-M400 was higher than CB-P. This may be because the CB-P component's organic chemical structure was damaged by the Pb (II) ions.

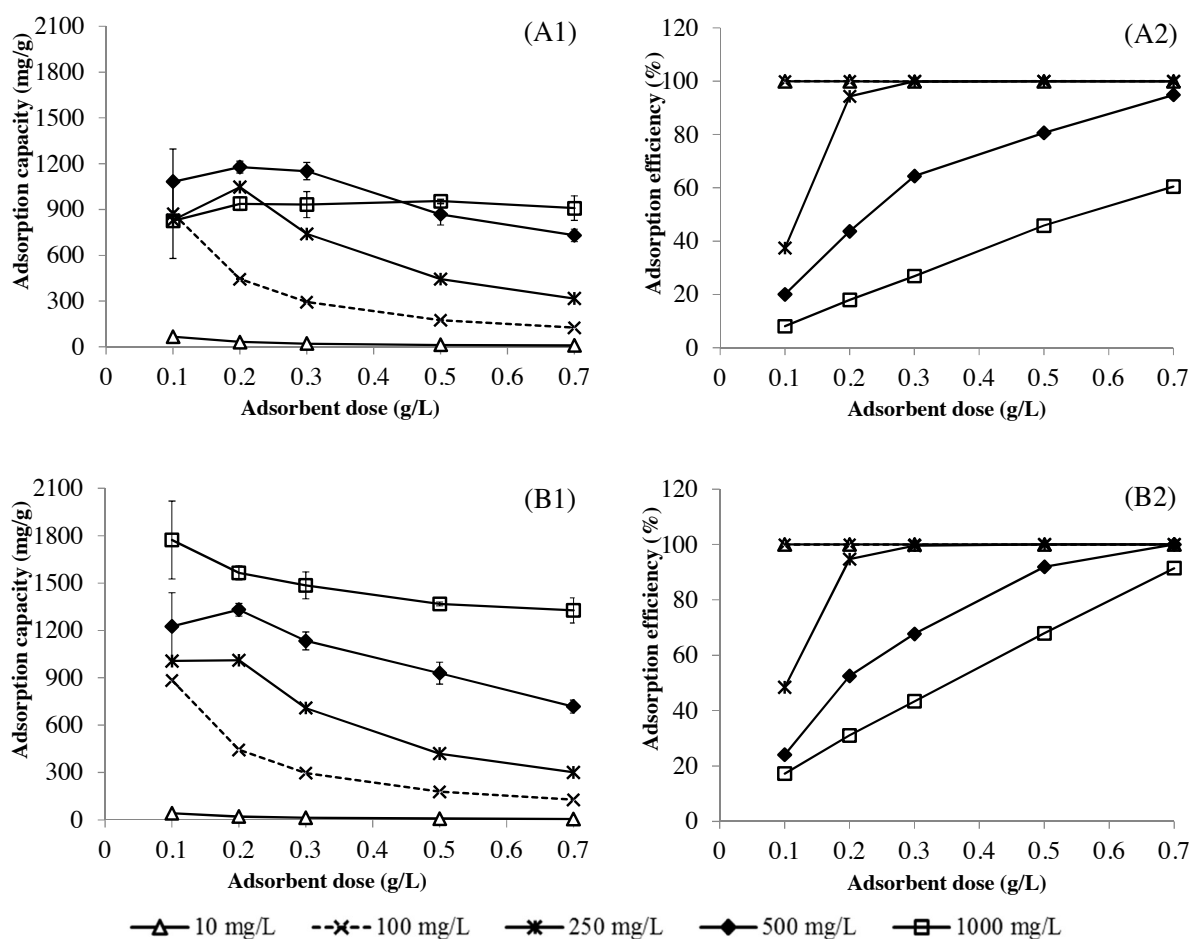


Figure 4. Effect of adsorbent doses (0.1-0.7 g/L) and initial Pb (II) concentrations (10-1000 mg/L) from the batch experiments at an initial pH of 4.0 during 240 min of contact time. (A1) and (A2) represent the adsorption capacity (mg/g) and efficiency (%) of CB-P, respectively. (B1) and (B2) represent the adsorption capacity (mg/g) and efficiency (%) of CB-M400, respectively

Table 3. Parameters of Pb (II) adsorption isotherm onto CB-P and CB-M400

Adsorbent	Langmuir isotherm			Freundlich isotherm		
	$q_m$ (mg/g)	$K_L$	$R^2$	$n$	$K_F$	$R^2$
CB-P	869.57	-0.1217	0.9329	15.67	657.7	0.5434
CB-M400	1573.56	0.0705	0.9724	9.60	732.8	0.7512

### 3.4 Adsorption isotherm

Adsorption equilibrium, described via the adsorption isotherm, was used to evaluate maximum adsorption capacity of Pb (II). The Pb (II) adsorptions of CB-P and CB-M400 were fixed with Langmuir's isotherm ( $R^2 = 0.9329-0.9724$ ) to a greater degree than Freundlich's isotherm ( $R^2 = 0.5434-0.7512$ ). The isotherm parameters are included in Table 3. From Langmuir's isotherm, the maximum adsorption capacity ( $q_m$ ) of CB-M400 was 1573.56 mg/g, which was higher than CB-P's at 869.57 mg/g. As a result, although the surface area of CB-M400 was less than that of CB-P, its maximum adsorption capacity was greater than that of CB-P. This suggests that other factors besides the sorbent surface affect the adsorption of Pb (II) from the aqueous solution. In this study, the calcite component of  $\text{CaCO}_3$  in CB-M400 may play a regulating role in Pb (II) removal. Du *et al.* (2011) reported that the aragonite and calcite in  $\text{CaCO}_3$  showed different adsorption capacities for heavy metals.

According to Langmuir's isotherm assumption, the adsorption behavior of CB-P and CB-M400 Pb (II) is characterized by a monolayer adsorption at a fixed number of identical and equivalent active sites

(Febrianto *et al.*, 2009; Foo and Hameed, 2010). The key mechanism of  $\text{CaCO}_3$  composite materials' Pb (II) adsorption is carbonate microprecipitation on the surface; here, the precipitates are adsorbed by the chitin or organic matter (Lee *et al.*, 1997; Vijayaraghavan and Joshi, 2013). Moreover, an ion exchange process between metal and Ca on the adsorbent occurs in Cu (II) adsorption via cuttlebone adsorbent (Li *et al.*, 2010). The carbonaceous properties of CB-M400 could function as organic matter in CB-P for Pb (II) adsorption, as the carbonate precipitates adsorption with higher efficiency in low pH and high Pb (II) concentrations.

The maximum adsorption capacities of CB-P and CB-M400 were compared to adsorbents that were examined in previous studies (Table 4). Compared to other  $\text{CaCO}_3$  composites such as crab shells (Lee *et al.*, 1997; Ramalingam *et al.*, 2014) and eggshells (Vijayaraghavan and Joshi, 2013), adsorbents from cuttlebones has a comparable Pb (II) uptake capacity. However, the CB-P and CB-M400 in this study were found to be more effective for Pb (II) removal than other adsorbents. Thus, the present study illustrates the potential for using CB-P and CB-M400 to remove Pb (II) from wastewater.

Table 4. Comparison of the maximum adsorption capacities ( $q_m$ ) of different adsorbents to Pb (II) reported in literatures.

Adsorbent	pH	$q_m$ (mg/g)	Reference
<i>Corallina mediterranea</i> (Red algae)	5.0	64.30	(Ibrahim, 2011)
<i>Galaxaura oblongat</i> (Red algae)	5.0	88.60	(Ibrahim, 2011)
<i>Jania rubens</i> (Red algae)	5.0	30.60	(Ibrahim, 2011)
<i>Pterocladia capillacea</i> (Red algae)	5.0	34.10	(Ibrahim, 2011)
<i>Ulva lactuca</i> sp. (Green algae waste)	5.0	56.01	(Bulgariu and Bulgariu, 2012)
<i>Cystoseira barbata</i> (Brown algae)	4.0	246.98	(Tang <i>et al.</i> , 2013)
<i>Lemna perpusilla</i> Torr. (Minute duckweed)	4.6	128.21	(Yalçin <i>et al.</i> , 2012)
Chicken eggshell powder	5.0	577	(Vijayaraghavan and Joshi, 2013)
<i>P. sanguinolentus</i> (Crab shell)	4.0	714	(Ramalingam <i>et al.</i> , 2014)
<i>P. trituberculatus</i> (Crab shell)	5.0	1,300	(Lee <i>et al.</i> , 1997)
CB-P	4.0	869.57	This study
CB-M400	4.0	1,573.56	This study

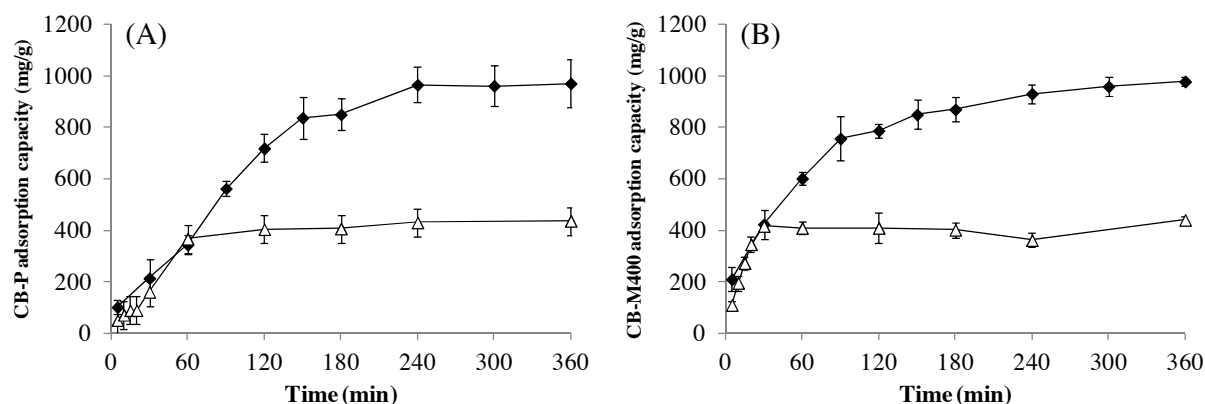


Figure 5. Pb (II) adsorption capacity from 0-360 min with concentrations of 100 mg/L ( $\triangle$ ) and 500 mg/L ( $\blacklozenge$ ) and an initial pH of 4.0 using an adsorbent dose of 0.2 g/L. (A) CB-P, (B) CB-M400

### 3.5 Adsorption kinetic

The results of the kinetic experiment indicated the adsorption equilibrium time and reaction rate of Pb (II) removal of the biosorbents. The Pb (II) adsorption capacities from 0-360 min are presented in Fig. 5. In the Pb (II) 100 mg/L load, the Pb (II) adsorption of CB-P and CB-M400 was rapid: 80-90% removal in 30 and 60 min, respectively. After this, it slowly increased until it plateaued and became unchanging when the adsorption reaction reached equilibrium. The initial fast Pb (II) sorption of CB-P and CB-M400 was due to the large available surface area of the sorbents, which were gradually covered with the surface precipitate  $\text{PbCO}_3$  with prolonged contact time. The adsorption capacity of the Pb (II) 500 mg/L load was higher than the Pb

(II) 100 mg/L load and took longer to reach equilibrium. Pseudo first-order and pseudo second-order kinetic models were used to estimate adsorption rates (Febrianto *et al.*, 2009). The pseudo second-order model ( $R^2 = 0.9241$ - $0.9710$  for CB-P and  $R^2 = 0.9867$ - $0.9958$  for CB-M400) predicted kinetic data better than the pseudo first-order model ( $R^2 = 0.8965$ - $0.9435$  for CB-P and  $R^2 = 0.1736$ - $0.9921$  for CB-M400) and had a high correlation coefficient (Table 5). Moreover, the pseudo second-order rate constant ( $k_2$ ) correlated to a high adsorption rate in CB-M400 at the same initial concentration (Table 5). The pseudo second-order kinetic model was based on the fact that the rate-limiting step is controlled by chemisorption. The good fit with the pseudo second-order kinetic model suggests that chemisorption occurred in the sorption process (Du *et al.*, 2011).

Table 5. Parameters of adsorption kinetic model of Pb (II) onto CB-P and CB-M400 at different initial metal concentrations

Adsorbent	Pb (II) (mg/L)	psuedo-first order			psuedo-second order		
		$k_1$ (1/min)	$q_e$ (mg/g)	$R^2$	$k_2$ (g/mg/min)	$q_e$ (mg/g)	$R^2$
CB-P	100	0.0173	395.12	0.9435	$3.06 \times 10^{-5}$	528.82	0.9710
	500	0.0180	1565.09	0.8965	$6.41 \times 10^{-6}$	1340.12	0.9241
CB-M400	100	0.0048	109.74	0.1736	$2.50 \times 10^{-4}$	434.78	0.9867
	500	0.0120	778.21	0.9921	$2.39 \times 10^{-5}$	1075.62	0.9958

$q_e$  is the adsorption capacity at equilibrium,  $k_1$  and  $k_2$  are the pseudo first and second-order equilibrium rate constant



#### 4. Conclusion

The present study used cuttlebone as a biosorbent for Pb (II) removal with a combination of microprecipitation adsorption and ion exchange processes; it proved itself to be an effective biosorbent. CB-P and CB-M400 surfaces before adsorption were observed to have a rough structure with highly porous surfaces, whereas after the biosorbents were treated with a Pb (II) solution, Pb crystals were adsorbed and appeared to cover the surface. The maximum Pb (II) adsorption capacity in the aqueous solution with the optimum condition at pH 4.0 and a biosorbent dose of 0.2 g/L were 869.57 mg/g in CB-P and 1,573.56 mg/g in CB-M400. Although CaCO<sub>3</sub> is the main factor in the Pb (II) adsorption process using cuttlebone as a biosorbent, this study found that its adsorption capacity and adsorption rate can be enhanced by modifying the organic carbon in CB-P into a fixed carbon in CB-M400 via a carbonization process. Therefore, low cost, rapid and high adsorptive ability of cuttlebone would offer a promising technique for industrial wastewater treatment.

#### Acknowledgements

The authors extended acknowledges to Department of Environmental Science Faculty of Science, Chulalongkorn University. Special thanks are gratefully expressed to Scientific and Technological Research Equipment Centre of Chulalongkorn University.

#### References

- Baby J, Raj JS, Biby ET, Sankarganesh P, Jeevitha MV, Ajisha SU, Rajan SS. Toxic effect of heavy metals on aquatic environment. *International Journal of Biological and Chemical Sciences* 2010; 4(4): 939-52.
- Bailey SE, Olin TJ, Bricka RM, Adrian DD. A review of potentially low-cost sorbents for heavy metals. *Water Research* 1999; 33(11): 2469-79.
- Ben Nasr A, Walha K, Charcosset C, Ben Amar R. Removal of fluoride ions using cuttlefish bones. *Journal of Fluorine Chemistry* 2011; 132(1): 57-62.
- Birchall JD, Thomas NL. On the architecture and function of cuttlefish bone. *Journal of Materials Science* 1983; 18(7): 2081-86.
- Boonamnuayvitaya V, Chaiya C, Tanthapanichakoon W, Jarudilokkul S. Removal of heavy metals by adsorbent prepared from pyrolyzed coffee residues and clay. *Separation and Purification Technology* 2004; 35(1): 11-22.
- Bulgariu D, Bulgariu L. Equilibrium and kinetics studies of heavy metal ions biosorption on green algae waste biomass. *Bioresource Technology* 2012; 103(1): 489-93.
- Chen X, Chen G, Chen L, Chen Y, Lehmann J, McBride MB, Hay AG. Adsorption of copper and zinc by biochars produced from pyrolysis of hardwood and corn straw in aqueous solution. *Bioresource Technology* 2011; 102(19): 8877-84.
- Demirbas A, Arin G. An overview of biomass pyrolysis. *Energy Sources* 2002; 24(5): 471-82.
- Du Y, Lian F, Zhu L. Biosorption of divalent Pb, Cd and Zn on aragonite and calcite mollusk shells. *Environmental Pollution* 2011; 159(7): 1763-68.
- Febrianto J, Kosasih AN, Sunarso J, Ju YH, Indraswati N, Ismadji S. Equilibrium and kinetic studies in adsorption of heavy metals using biosorbent: a summary of recent studies. *Journal of Hazardous Materials* 2009; 162(2-3): 616-45.
- Florek M, Fornal E, Gómez-Romero P, Zieba E, Paszkowicz W, Lekki J, Nowak J, Kuczumow A. Complementary microstructural and chemical analyses of *Sepia officinalis* endoskeleton. *Materials Science and Engineering: C* 2009; 29(4): 1220-26.
- Foo KY, Hameed BH. Insights into the modeling of adsorption isotherm systems. *Chemical Engineering Journal* 2010; 156(1): 2-10.
- Fu F, Wang Q. Removal of heavy metal ion from wastewaters: a review. *Journal of Environmental Management* 2011; 92(3): 407-18.
- Hassan A, Kaewsichan L. Removal of Pb(II) from aqueous solutions using mixtures of bamboo biochar and calcium sulphate, and hydroxyapatite and calcium sulphate. *EnvironmentAsia* 2016; 9(1): 37-44.
- Ibrahim WM. Biosorption of heavy metal ions from aqueous solution by red macroalgae. *Journal of Hazardous Materials* 2011; 192(3): 1827-35.
- Kadirvelu K, Thamaraiselvi K, Namasivayam C. Removal of heavy metals from industrial wastewaters by adsorption onto activated carbon prepared from an agricultural solid waste. *Bioresource Technology* 2001; 76(1): 63-65.
- Khalid N, Rahman S. Adsorptive removal of lead from battery wastewater by coconut coir. *Separation Science and Technology* 2010; 45(14): 2104-12.
- Klungsuwan P, Jarerat A, Poompradub S. Mechanical properties and biodegradability of cuttlebone/NR composites. *Journal of Polymers and the Environment* 2013; 21(3): 766-79.
- Lee MY, Park JM, Yang JW. Micro precipitation of lead on the surface of crab shell particles. *Process Biochemistry* 1997; 32(8): 671-77.
- Li H, Jin D, Li R, Li X. Structural and mechanical characterization of thermally treated conch shells. *JOM* 2015; 67(4): 720-25.
- Li YZ, Pan H, Xu J, Fan XW, Song XC, Zhang Q, Xu J, Liu Y. Characterization of metal removal by os sepiae of *Sepiella maindroni* Rochebrune from aqueous solutions. *Journal of Hazardous Materials* 2010; 179 (1-3): 266-75.
- Mudhoo A, Garg VK, Wang S. Removal of heavy metals by biosorption. *Environmental Chemistry Letters* 2012; 10(2): 109-17.

- Ramalingam S, Parthiban L, Rangasamy P. Biosorption modeling with multilayer perceptron for removal of lead and zinc ions using crab shell particles. *Arabian Journal for Science and Engineering* 2014; 39(12): 8465-75.
- Sandesh K, Suresh Kumar R, JagadeeshBabu PE. Rapid removal of cobalt (II) from aqueous solution using cuttlefish bones; equilibrium, kinetics, and thermodynamic study. *Asia-Pacific Journal of Chemical Engineering* 2013; 8(1): 144-53.
- Tang Y, Chen L, Wei X, Yao Q, Li T. Removal of lead ions from aqueous solution by the dried aquatic plant, *Lemna perpusilla* Torr. *Journal of Hazardous Materials* 2013; 244-245: 603-12.
- Vijayaraghavan K, Joshi UM. Chicken eggshells remove Pb (II) ions from synthetic wastewater. *Environmental Engineering Science* 2013; 30(2): 67-73.
- Wan Ngah WS, Hanafiah MA. Removal of heavy metal ions from wastewater by chemically modified plant wastes as adsorbents: a review. *Bioresource Technology* 2008; 99(10): 3935-48.
- Wang SY, Tsai MH, Lo SF, Tsai MJ. Effects of manufacturing conditions on the adsorption capacity of heavy metal ions by Makino bamboo charcoal. *Bioresource Technology* 2008; 99(15): 7027-33.
- Yadanaparthi SKR, Graybill D, von Wandruszka R. Adsorbents for the removal of arsenic, cadmium, and lead from contaminated waters. *Journal of Hazardous Materials* 2009; 171(1-3): 1-15.
- Yalçın S, Sezer S, Apak R. Characterization and lead (II), cadmium(II), nickel(II) biosorption of dried marine brown macro algae *Cystoseira barbata*. *Environmental Science and Pollution Research* 2012; 19(8): 3118-25.

---

Received 2 August 2016

Accepted 5 September 2016

#### Correspondence to

Dr. Sarawut Srithongouthai  
Department of Environmental Science,  
Faculty of Science,  
Chulalongkorn University,  
Phayathai Road,  
Bangkok 10330,  
Thailand  
Tel: +66-2-218-5194  
Fax: +66-2-218-5180  
E-mail: sarawut.sr@chula.ac.th